https://erjm.journals.ekb.eg
ISSN: 2210-1219

DOI: ---------

ERJ
Engineering Research Journal
Faculty of Engineering
Menoufia University

Improvement the Efficiency of the Connections Between Circular Columns and End-Plate

Ahmed M. Abd El-ghany[1*], Boshra A. Eltaly[2], Mahmoud S. Elnagar[2] and Kamel S. Kandeel[2*]

[1] *PhD Candidate, Department of Civil Engineering, Faculty of Engineering, Menoufia University, Egypt.*

[2] *Department of Civil Engineering, Faculty of Engineering, Menoufia University, Egypt.*

**(engahmedmontaser87@gmail.com)*

ABSTRACT

The goal of this study is to look into a new low-cost connection that can be readily established on the site. Similarly, to improve the efficiency of the connections and investigate the various variables that influence their capacity. Several studies focused on the behavior of these connections under various types of loads, which led to the discovery of their weak points, the ideal strength method for these connections under various loads, the best method of erection, as well as the cost and the time of construction. In the research's experimental part, a vertical force was applied to three types of connections between a circular column and end-plate. The connection was strengthened by filling the column with concrete and welding two circular bars in the tension and compression zones. The tested connections were analyzed using a computer program in the numerical analysis section (ANSYS 16). Finite element results were validated with experimental results. The parametric study of six extended end-plate connections separated into two groups under the effect of shearing force. The use of two internal circular bars at the tension and compression zones and the filling of the column with concrete are the main parameters that are considered in the study.

Keywords: *End-plate connections; circular column; composite section; Moment rotation curve; Finite element analysis.*

1. Introduction

The behavior of connections has a big impact on the structure's overall behavior. In this context, evaluating the actual response of steel connections, particularly welded end-plate connections, has been a major focus of research for more than a decade. End-plate connectors have several advantages, including cost, ease of manufacture, and structural performance [1–5]. Previously, the most well-known phrases to describe joint activity were stiff joint and pin joint. Recently, a term known as semi-rigid connections [6] has been coined to describe the relationship between them.

The graph of the bending moment (M) versus the appropriate rotation) (and its properties) are important tools for representing semi-rigid connections. Experiments, numerical analysis, and analytical models are common ways for obtaining this relationship. The validity of the second and third methods was obtained from the first method's calibration or both. Many research employed regression analysis to represent quantitatively the moment rotation curve characteristics such as linear, bi-linear, multi-linear, exponential functions, polynomial functions, B-spline, power function, Richard-Abbott, and RambergOsgood function [7–12]. To identify the properties of the M– curve, Mofid et al. [13, 14], Mohamadi-Shoreh and Mofid [15], and Shi et al. [16] employed analytical analysis and mathematical expressions based on plate theory, yield line theory, and the virtual work technique to determine the characteristics of the M–θ curve.

The ability to obtain data as well as the good representation of the materials' nonlinear effects, contact, and sliding between connection elements distinguished the finite element model FEM using a software program such as ANSYS and ABAQUS. For the parametric analysis of end-plate connections, the finite element method was the best option. To examine end-plate connections, most previous research relied on calibrated FEM with experimental results [17–23].

Cheng et al. [27] investigated experimentally and numerically new connection system for circular tubed reinforced concrete (TRC) columns and steel beams with crossing diaphragms. Mou [28] conducted experimental investigation on the seismic behavior of a novel connection between a beam and a reinforced concrete-filled steel tube (RCFST) column. The connection was tested under cyclic loading to evaluate the failure modes, hysteretic performance, stiffness degradation, strength degradation, energy dissipation capacity and the strain responses. Fan and Zhao [29] studied experimentally and numerically connection between concrete-filled double-skin steel tubular (CFDST) column and steel beam with flush endplates and bidirectional bolts.

The bending moment about the strong axis of the connections was considered in the earlier investigations, as summarized above. This work aims to better understand the behavior of connections subjected to bending moment under the effect of static load, as well as the effect of reinforcing the connection by filling the column with concrete and welding two circular bars in the tension and compression zones. Three extended endplates steel beam-to-column connections were subjected to bending moment under the action of static load up to failure in an experimental program. In addition, FEM was used with the ANSYS program and calibrated with the experimental data of test results. The goal of this paper is to investigate the effect of bending moment under the effect of static load on the characteristics of the load-deflection curve. In addition, the paper presents a calibrated FEM model that can make an extensive study for these connections, and determine the main effective parameters to carry out an extensive parametric study as a second step of the strengthening techniques of the connection by filling the column with concrete and welding two circular bars in the tension and compression zones.

2. Experimental Program

The most frequent connection used to link the beam to the tubular column for structures is an end plate steel connection. When a beam is loaded, it receives a vertical load from the structure's weight, as well as its own weight and the live load. The connection is subjected to bending moment and shear force in this case. When it comes to designing these connections, there is a knowledge gap. Three specimens of end plate steel connections between the cantilever beam and column were tested under the action of a vertical load with 250 mm eccentricity. Figures (1, 2 and 3) and Table 1 exhibit details and descriptions of the specimens. The cantilever form of the connection is one of the most frequent configurations for determining the behavior of the connections, and it was employed in a number of previous studies, including [1, 12, 20 and 24] and others. The most significant advantages of this design are its low cost, ease of production and implementation, and suitability for testing in laboratories.

The specimens are end-plate connections with constant geometry except for end-plate thickness (tp), column diameter (D), and column thickness (tc). The tubular column has a diameter of 219.1 mm, thickness 6 mm and a length of 1,000 mm. The end plate has a cross-section of 300 × 250 × 13 mm. The Gas Metal Arc Welding (GMAW) technology was used to assemble all of the column's components as well as the cantilevers end plate. End plates are welded to the column. The shear and bearing strength of the connections were developed to resist the shear force, with the semi rigid joint as the connection type. The samples had two variables: first, the column was filled with concrete, and second, two internal circular bars with a diameter of 16 mm were placed in the tension and compression zones.

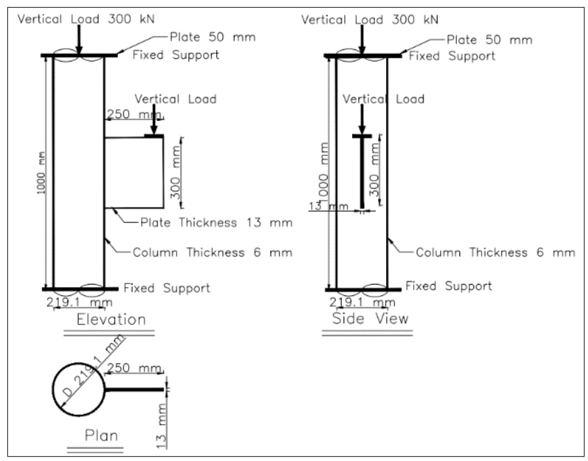

Figure 1- Details of specimen CC 6-6

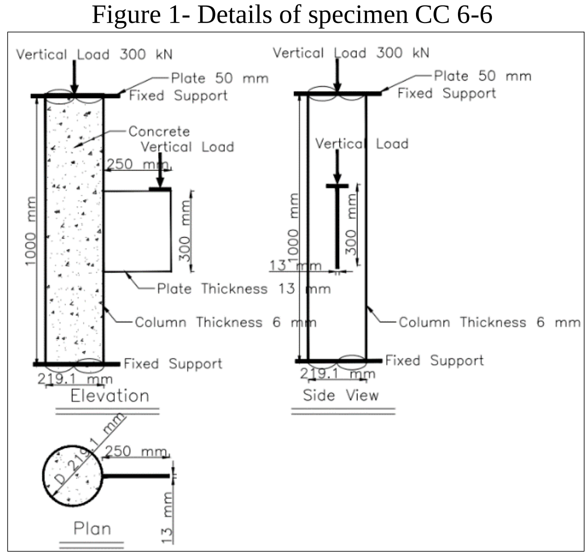

Figure 2- Details of specimen CWC 6-6

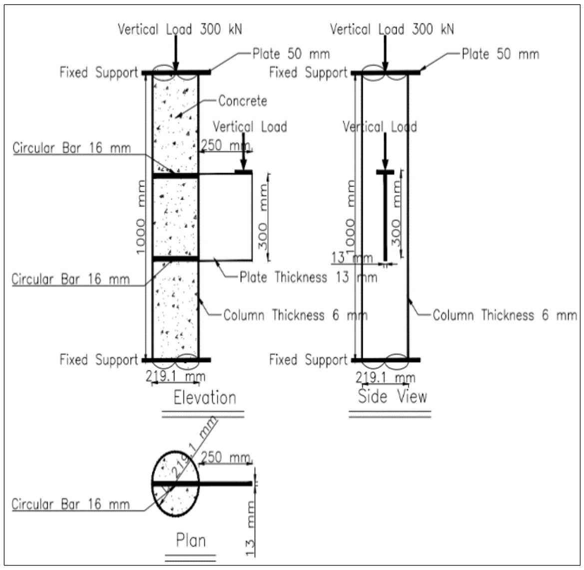

Figure 3- Details of specimen CWCB 6-6

Table 1- Description of specimens

Test ID	Composite	Internal bar
CC 6-6	-	-
CWC 6-6	√	-
CWCB 6-6	√	√

3.1 Properties of the Used Materials

The cement used in this study was Egyptian regular Portland cement with a hardness of 52.5 N. The coarse and fine aggregates used in the experimental work were readily available on the market (dolomite and sand). For the aggregate, sieve analyses were performed, and the findings were recorded and compared to the Egyptian Standard Specifications (E.S.S.) 2021 [9]. Electrical concrete mixer was used to cast all of the samples. The normal cube compressive strength reached 25 MPa after 28 days of curing. The column and end-plate have a tensile strength of 370 MPa (ST 37). The column and end-plate have a yield strength of 300 MPa (ST 37).

The strengthened connections were coded as (CWC 6-6 and CWCB 6-6) in the first sample, which was strengthened by filling the column with concrete, and in the second sample, which was strengthened by filling the column with concrete and but two circular bar 16 mm in the tension and compression zones, as shown in Fig. (3 and 4). Fig. 5 presents the sample before the test.

3.2 Test Setup and Instrumentation

The experiment was carried out at Tanta University's Reinforced Concrete and Heavy Structures Lab in the Structural Engineering Department. The specimen setup and instrumentation distribution are shown in Fig. 9. Four M20 bolts with Grade 8.8a were used to secure the column base to the laboratory frame, as shown in Fig. 6. As illustrated in fig. 7, the top end was held by a vertical load of 303 kN and a circular ring to prevent the column from moving horizontally. To create bending moments on the connections, vertical load (PV) cells were supported at the end of the end-plate. Four Linear Variable Displacement Transducers (LVDTs) were used to measure the required displacements as shown in Fig. 8.

Figure 4- preparing of connection

Figure 5- Pictures for the sample before the test

Figure 6- Lower fixed support

Figure 7- Upper fixed support

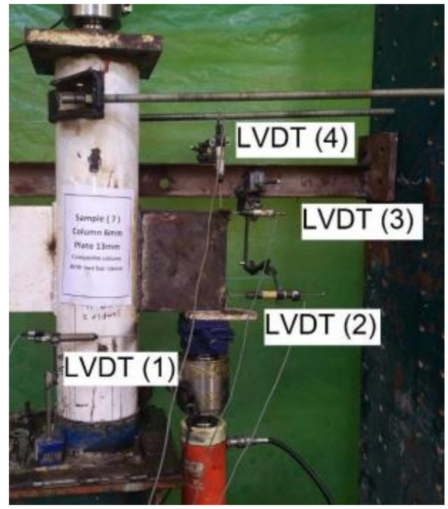

Figure 8- LVDT number and position

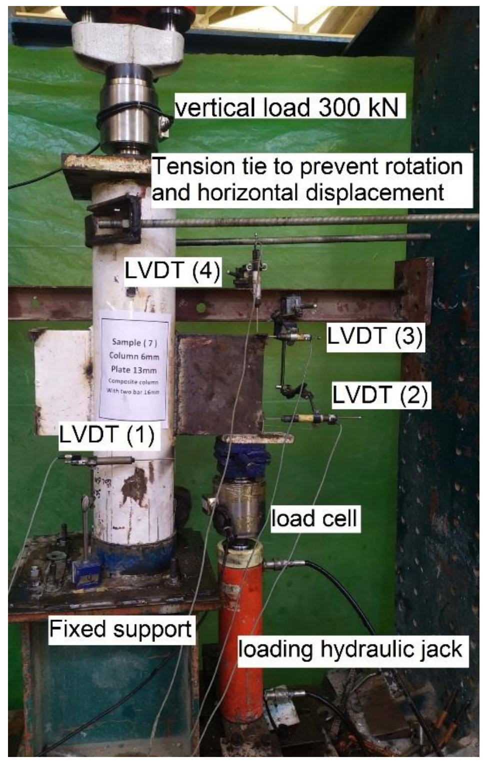

Figure 8- Test Setup

3.3 Testing Procedure

Electronic recording started and all the equipment was verified. As illustrated in Fig. 7, the test was initiated by providing a persistent load of 300 kN at the middle of the column during the test. Then, all of the recorded readings were set to zero. Up until failure, the specimens were subjected to a constant vertical force. The loading technique involves the application of a specified vertical load for specimen's subject to bending moment. This method was carried out until it collapsed. The presentation and discussion of test findings were combined with the corresponding results from the FEM in Sec. III.

4. Finite Element Simulation

ANSYS workbench, a general-purpose Finite Element (FE) analysis tool, was used to create a numerical 3D model. As illustrated in Fig. 10, all elements of the connections (column, end-plates, concrete, circular bar and welds) were meshed using the multizone mesh method and modelled using the 8-nodes solid structural element SOLID185. The Multi-Zone mesh method, which is a patch-independent meshing methodology, decomposes geometry into mapped (structured/sweepable) and free (unstructured) regions automatically. Where possible, it constructs a pure hexahedral mesh and then fills the more difficult-to-capture parts with an unstructured mesh. The SOLID185 element can be used to model two types of 3D solid structures: homogeneous and layered structures. It is made up of eight nodes, each with three degrees of freedom (translation in three global axes directions). Plasticity, hyperelasticity, stress stiffening, creep, huge deflection, and big strain capabilities can all be defined with this element [25]. Surface-to-surface contact elements TARGE170 and CONTA173 were used to specify the contact between each pair of adjacent parts. Between the column and the filled concrete, friction contact with a friction coefficient of 0.2 was imposed. Other sections, such as the end-plate and column, the internal bar and column, and the internal bar and concrete, all had bonded contact. The Multilinear Kinematic Hardening assumption, according to Azap [26], was used to depict the nonlinear stage of the stress strain curve, and it produced good results. Newton–Raphson method was used to make force convergence and large deflection was defined.

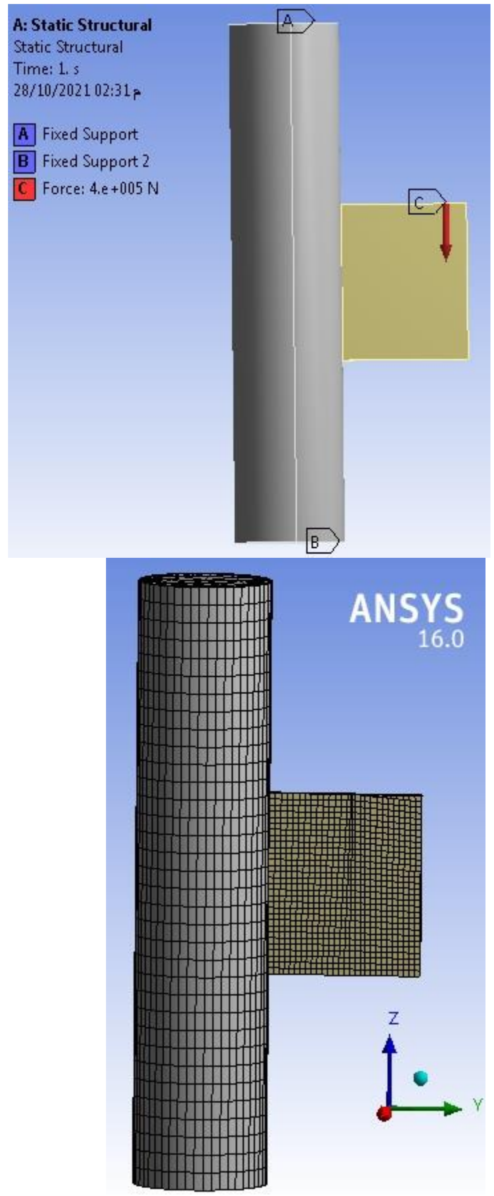

Figure 7- General view of the FE model (Boundary conditions and elements meshes)

5. Results

The deformations of the three specimens were displayed and discussed in this section. The experimental and FEM data are contrasted and analyzed in terms of determining and plotting load-displacement curves and their properties. The strong axis of the connections was used to determine all curves and attributes. By comparing the features of the control sample connections under the effect of bending moment and shear force and discussing the differences, the effect of the concrete filling and internal circular bar on the connection's behavior was investigated. The approach increased ultimate load, stiffness, and decreased ductility of the connection, as shown in this graph. The load-displacement curve produced from the FE model and experimental test results for three samples at four LVDTs are shown in Figures 11–14.

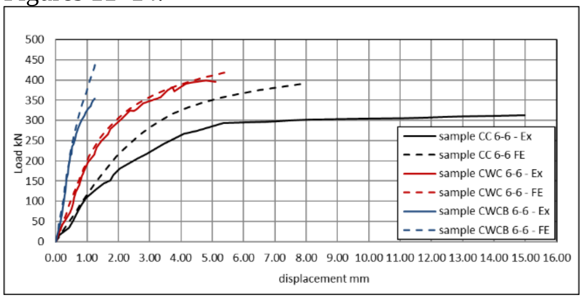

Figure 11- load-displacement curves of the FE and experimental results at LVDT (1)

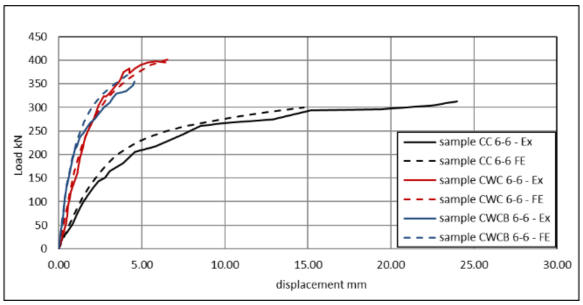

Figure 12- load-displacement curves of the FE and experimental results at LVDT (2)

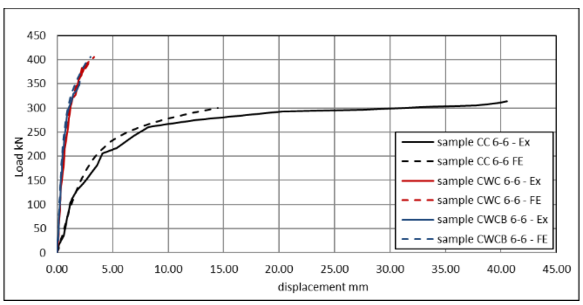

Figure 13- load-displacement curves of the FE and experimental results at LVDT (3)

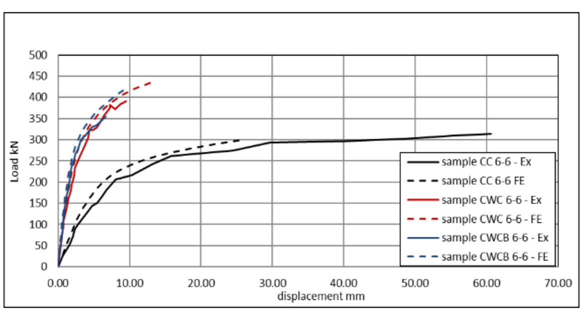

Figure 14- load-displacement curves of the FE and experimental results at LVDT (4)

The deformed shape of the end-plates and the column at the end of the test due to the experimental testing and the FEM is shown in Fig.15 to 23. Contact between the end-plate and the column increased and decreased deformation at tension and compression for the connections subjected to vertical load (CWC 6-6, and CWCB 6-6). According to testing results, CWC 6-6 and CWCB 6-6 specimens reduce maximum applied vertical load and total horizontal displacement at LVDT (1) by 61.58 percent and 93.1 percent, respectively. According to finite element data, CWC 6-6 and CWCB 6-6 specimens reduce maximum applied vertical load and total horizontal displacement at LVDT (1) by 54.76 percent and 92.24 percent, respectively. According to testing data, CWC 6-6 and CWCB 6-6 specimens reduce maximum applied vertical load and total horizontal displacement at LVDT (2) by 52.63 percent and 58.95 percent, respectively. According to finite element data, CWC 6-6 and CWCB 6-6 specimens reduce maximum applied vertical load and total horizontal displacement at LVDT (2) by 55.39 percent and 60.96 percent, respectively. According to testing results, the CWC 6-6 and CWCB 6-6 specimens reduce the maximum applied vertical load and total horizontal displacement at LVDT (3) by 76.65% and 88.54 percent, respectively. As the finite element data, the CWC 6-6 and CWCB 6-6 specimens reduce maximum applied vertical load and total horizontal displacement by 73.5 percent and 78.58 percent at LVDT (3), respectively. As the testing results, the CWC 6-6 and CWCB 6-6 specimens reduce maximum applied vertical load and total horizontal displacement at LVDT (4) by 61.45 percent and 75.69 percent, respectively. According to the finite element data, the CWC 6-6 and CWCB 6-6 specimens reduce maximum applied vertical load and total horizontal displacement at LVDT (4) by 63.91 percent and 70.84 percent, respectively.

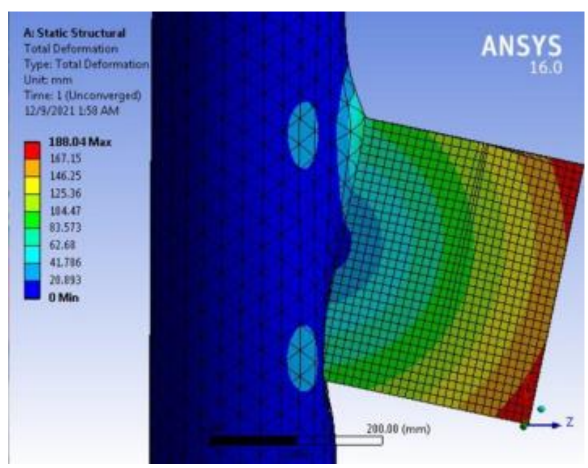

Figure15- Numerical Deformed Shape for CC 6-6

Figure 16- Experimental Deformed Shape for CC 6-6

Compression Failure Tension Failure

Figure 17- Description of specimen deformations for CC 6-6

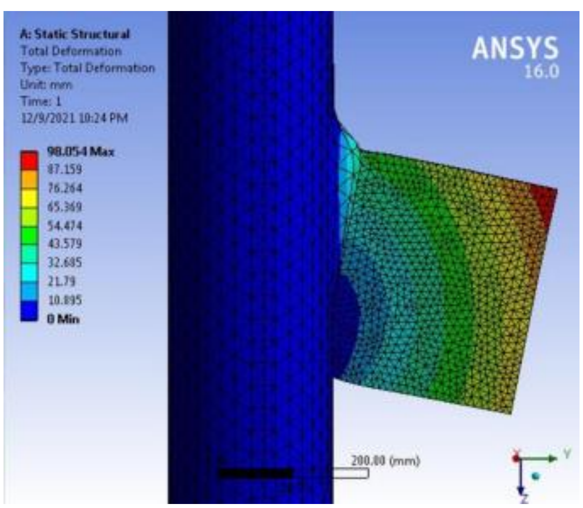

Figure 18- Numerical Deformed Shape for CWC 6-6

Figure 19- Deformed Shape for CWC 6-6

Figure 20- Deformed Shape for CWC 6-6

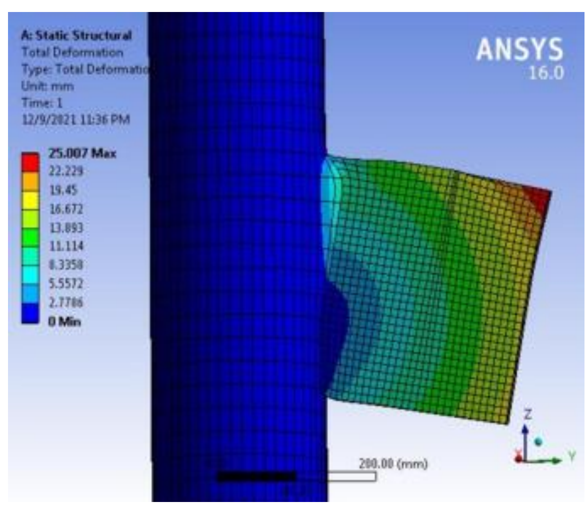

Figure 21- Numerical Deformed Shape for CWCB 6-6

Figure 22- Deformed Shape for CWCB 6-6

Figure 23- Deformed shape for CWCB 6-6

5. Parametric Study

The effect of concrete and internal circular bar on the principal characteristics of the extended endplate connections was studied as a parametric analysis using the calibrated FEM. The focus of the research is on the behavior of the end-plate under the influence of the bending moment. The experimental and numerical analyses revealed that filling the circular column with concrete and placing two circular bars 16 mm in the tension and compression zones strengthened the connection between the end-plate and the circular column.

Table 2- Summarized the numerical models group (1)

Specimen ID	Studied parameters	Filled with concrete	Internal circular bar diameter
CWCB 6-6	Reference specimen	C 25	16 mm
CWCB 6-6 Ø12	difference diameter of internal bar	C 25	12 mm
CWCB 6-6 Ø18		C 25	18 mm
CWCB 6-6 Ø22		C 25	22 mm

Table 3- Summarized the numerical models group (2)

Specimen ID	Studied parameters	Filled with concrete	Internal circular bar
CWC 6-6	Reference specimen	C 25	-
CWC 6-6 c35	Difference young modulus of concrete	C 35	-
CWC 6-6 c45		C 45	-
CWC 6-6 c55		C 55	-

Mechanical parameters of internal round bar, concrete materials, and column diameters similar to those evaluated in the specimens were used to create numerical models (CC 6-6, CWC 6-6 and CWCB 6-6). The study's parameters are the young modulus of concrete filled the column and the diameter of the interior circular bar. The analyzed links were classified into two categories. As indicated in Table V (1), group (1) comprises three connections with the same column diameter but different internal circular bar diameters. As indicated in table V (2), group (2) has three connections with the same column diameter but different young modulus of concrete filled the column. The load-displacement curve produced from the FE model for group (1) at four LVDT are shown in Figures 24–27. The load-displacement curve produced from the FE model for group (1) at four LVDT are shown in Figures 28–31.

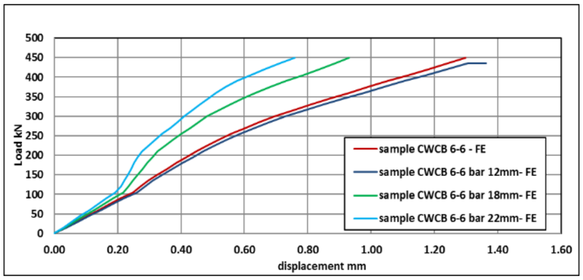

Figure 24- load vs displacement for specimens results at LVDT (1) at group (1)

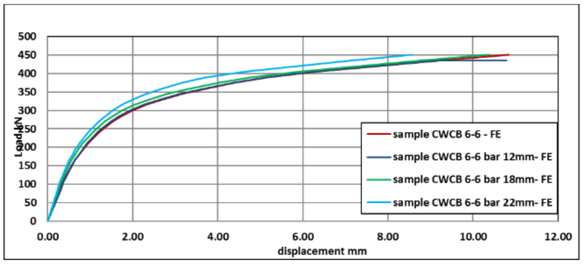

Figure 25- load vs displacement for specimens results at LVDT (2) at group (1)

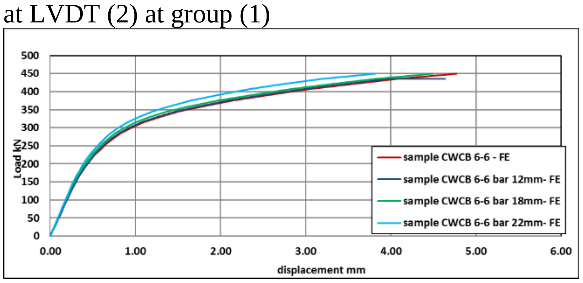

Figure 26- load vs displacement for specimens results at LVDT (3) at group (1)

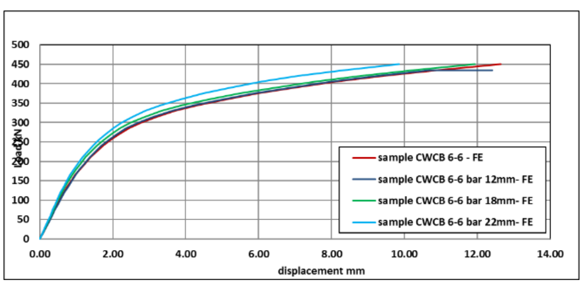

Figure 27- load vs displacement for specimen's results at LVDT (4) at group (1)

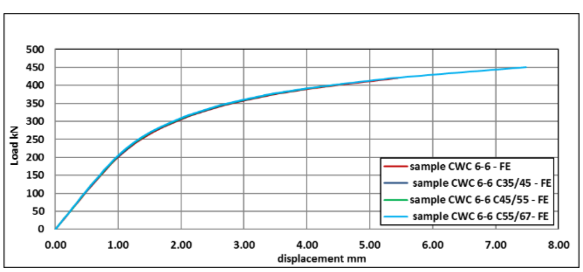

Figure 28- load vs displacement for specimen's results at LVDT (1) at group (2)

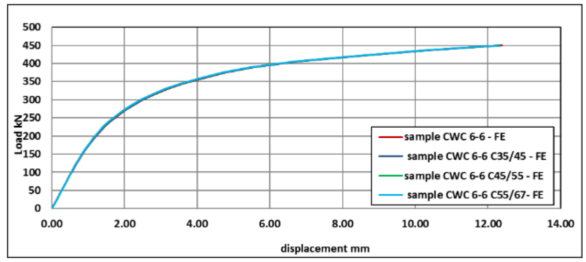

Figure 29- load vs displacement for specimen's results at LVDT (2) at group (2)

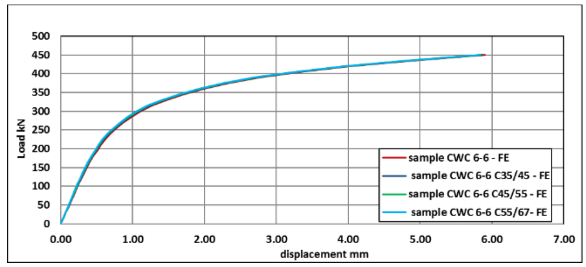

Figure 30- load vs displacement for specimens results at LVDT (3) at group (2)

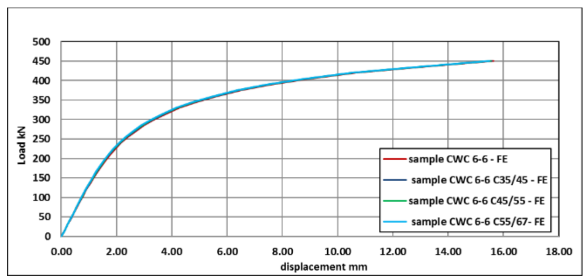

Figure 31- load vs displacement for specimen's results at LVDT (4) at group (2)

6. Conclusions

The effect of bending moment on the behavior of steel beam-to-column connections is discussed in this paper. Experiments on three extended end-plate connections were carried out under the influence of bending moment and shear force. The results of FEM using ANSYS software were compared to the results of the testing. The FEM includes material, contact, geometric nonlinearities, and sliding between the connection's parts. The major parameters evaluated and presented were the deformed shape and load-displacement curve of the connectors. The specimens were tested as part of a comprehensive experimental test. In addition, thorough numerical analyses were performed using the ANSYS 16 software. The FEA program was used to verify the results acquired from the generated analytical model. Parametric research was undertaken after validation against experimental data to investigate the parameters that affect the behavior of the connections between end plate and circular columns. The following conclusions can be taken from the discussion and comparisons of the results: -

1. Filling column with concrete can increase the behavior of the connections and decrease the deformation about range 52% to 76% at different measuring point.
2. The increasing of modulus of elasticity of filled concrete does not make perceptible effect at connection behavior.
3. The effect of filling the column with concrete and using two internal circular bars at one at the tension zone and one at the compression zone, can improve the efficiency of the connection by about 70% to 90% at the end of the elastic state.
4. The increasing internal circular bar diameter increases the rigidity of the contact area between column and end plate and decreases the horizontal displacement at this point, but it has a low effect on the total vertical displacement of the overall connection.

6. References

[1] Díaz C, Victoria M, Pascual M, Querin OM. FE model of beam-to-column extended end-plate joints. J Constr Steel Res 2011;67:1578–90.

[2] Fakih K, Chin SC, Doh SI. Behavior of extended end-plate steel beam-to-column connections. Open Civl Eng J 2018;12:250–62.

[3] Guo Z, Zhang X, Jia X. Behavior of endplate joints subjected to elevated temperature after cyclic loads. KSCE J Civil Eng 2018;22:4500–8.

[4] Yang R, Zhou X. Analysis of the mechanical behavior of bolted beam-column connections with different structural forms. Adv Civil Eng 2019;2019.

[5] Sarvestani HA. Parametric study of hexagonal castellated beams in post-tensioned self-centering steel connections. Front Struct Civil Eng 2019;13:1020–35.

[6] Hasan R, Kishi N, Chen WF, Komuro M. Evaluation of rigidity of extended endplate connections. J Struct Eng 1997;123(12):1595–602.

[7] Yee YL, Melchers RE. Moment-rotation curves for bolted connections. J Struct Eng 1986;112:615–35.

[8] Zhang A, Shangguan GH, Zhang YX, Wang QB, Cai WC. Experimental study of resilient prefabricated steel frame with all-bolted beam-to-column connections. Adv Steel Constr 2020;16(3):255–71.

[9] Attiogbe E, Morris G. Moment-rotation functions for steel connections. J Struct Eng 1991;117:1703–18.

[10] Sherbourne AN, Bahaari MR. Finite element prediction of end-plate bolted connection behavior I: Parametric study. J Struct Eng 1997;123:157–64.

[11] Sherbourne AN, Bahaari MR. Finite element prediction of end-plate bolted connection behavior II: Analytic formulation. J Struct Eng 1997;123:165–75.

[12] Abolmaalia A, Matthysa HJ, Farooqib M, Choic Y. Development of momentrotation model equations for flush end-plate connections. J Constr Steel Res 2005;61:1595–612.

[13] Mofid M, Ghorbani MA, McCabe SL. On the analytical model of beam-to-column semi-rigid connections, using plate theory. Thin-Walled Struct 2001;39:307–25.

[14] Mofid M, Mohammadi MRS, McCabe SL. Analytical approach on endplate connection: ultimate and yielding moment. J Struct Eng 2005;131(3):449–56.

[15] Mohamadi-Shoorea MR, Mofid M. Basic issues in the analytical simulation of unstiffened extended end-plate connection. Scientia Iranica 2004;11(4):303–11.

[16] Shi YJ, Chan SL, Wong YL. Modeling for moment-rotation characteristics for endplate connections. J Struct Eng 1996;122(11):1300–6. Maheri M. R. and Sahebi A. (1997) Use of steel bracing in reinforced concrete frames. Journal of Structural Engineering, 19(12): 1018-1024.

[17] Augusto H, da Silva LS, Rebelo C, Castrob JM. Characterization of web panel components in double-extended bolted end-plate steel joints. J Constr Steel Res 2016;116:271–93.

[18] Maggi YI, Gonçalves RM, Leon RT, Ribeiro LFL. Parametric analysis of steel bolted end-plate connections using finite element modelling. J Constr Steel Res 2005;61:689–708.

[19] Dessouki AK, Youssef AH, Ibrahim MM. Behavior of I-beam bolted extended endplate moment connections. Ain Shams Eng J 2013;4:685–99.

[20] Zeinoddini-Meimand V, Ghassemieh M, Kiani J. Finite element analysis of flush end-plate moment connections under cyclic loading. Int J Civil Environ Eng 2014;5(1):96–104.

[21] Parviz A, Ahadi P, Farajkhah V. Finite element analysis of extended stiffened

endplate link-to-column connections. Steel Constr 2016;9(1):46–57.
[22] Ismail RES, Fahmy AS, Khalifa AM, Mohamed YM. Numerical study on ultimate behavior of bolted end-plate steel connections. Latin Am J Solids Struct 2016;13:1–22.
[23] Shia G, Shia Y, Wang Y, Bradford MA. Numerical simulation of steel pretensioned bolted end-plate connections of different types and details. Eng Struct 2008;30:2677–86.
[24] Coelho AMG, Bijlaard FSK, da Silva LS. Experimental assessment of the ductility of extended end-plate connections. Eng Struct 2004;26:185–1206.
[25] ANSYS User Manual. Ansys Inc.
[26] Azap NM. Modelling of Nonlinear Behavior of Steel Beam to Column Semi-Rigid Connections with 3-D Solid Finite Elements. Master Thesis, Middle East Technical University, Turkey; 2013.
[27] Zhou X., Liu J., Cheng G., Gan D., and Chen Y. F., (2020) "New Connection System for Circular Tubed Reinforced Concrete Columns and Steel Beams," Engineering Structures, Vol. 214, p. 110666.
[28] Mou B., Liu X., and Sun Z., (2021) "Seismic Behavior of a Novel Beam to Reinforced Concrete-Filled Steel Tube Column Joint," Journal of Constructional Steel Research, Vol. 187, p. 106931.
[29] Fan J. and Zhao J., (2022) "Experimental Investigation and Analytical Modeling of Steel Beam-to-CFDST Column Connection," Journal of Constructional Steel Research., Vol. 190, p. 107164.